

UC Davis

UC Davis Previously Published Works

Title

Sortase-Mediated Phage Decoration for Analytical Applications

Permalink

<https://escholarship.org/uc/item/33z5b6nv>

Journal

Analytical Chemistry, 93(34)

ISSN

0003-2700

Authors

Ding, Yuan
Chen, He
Li, Jiao
et al.

Publication Date

2021-08-31

DOI

10.1021/acs.analchem.1c02322

Peer reviewed



Published in final edited form as:

Anal Chem. 2021 August 31; 93(34): 11800–11808. doi:10.1021/acs.analchem.1c02322.

Sortase-mediated phage decoration for analytical applications

Yuan Ding^{†,‡}, He Chen^{†,‡}, Jiao Li^{†,‡}, Lianrun Huang^{†,‡}, Guangyue Song^{†,‡}, Zhenfeng Li[§],
Xiude Hua^{*†,‡}, Gualberto Gonzalez-Sapienza[⊥], Bruce D. Hammock[§], Minghua Wang^{†,‡}

[†]College of Plant Protection, Nanjing Agricultural University, Nanjing 210095, China

[‡]State & Local Joint Engineering Research Center of Green Pesticide Invention and Application, Nanjing 210095, China

[§]Department of Entomology and UCD Cancer Center, University of California, Davis, CA 95616, United States

[⊥]Cátedra de Inmunología, Facultad de Química, Instituto de Higiene, Universidad de la República, Montevideo 11600, Uruguay

Abstract

Phage-borne peptides and antibody fragments isolated from phage display libraries have proven to be versatile and valuable reagents for immunoassay development. Due to the lack of convenient and mild-condition methods for the labeling of the phage particles, isolated peptide/protein affinity ligands are commonly removed from the viral particles and conjugated to protein tracers or nanoparticles for analytical use. This abolishes the advantage of isolating ready-to-use affinity binders and creates the risk of affecting the polypeptide activity. To circumvent this problem, we optimized the phage display system to produce phage particles that express the affinity binder on pIII and a polyglycine short peptide fused to pVIII that allows the covalent attachment of tracer molecules employing sortase A. Using a llama heavy chain only variable domain (VHH) against the herbicide 2,4-D on pIII as the model, we showed that the phage can be extensively decorated with a rhodamine-LPETGG peptide conjugate or the protein nanoluciferase (Nluc) equipped with a C-terminal LPETGG peptide. The maximum labeling amounts of rhodamine-LPETGG and Nluc-LPETGG were 1238 ± 63 and 102 ± 16 per phage, respectively. The Nluc-labeled dual display phage was employed to develop a phage bioluminescent immunoassay (P-BLEIA) for the detection of 2,4-D. The limit of detection and 50% inhibition concentration of P-BLEIA were 0.491 ng mL^{-1} and 2.15 ng mL^{-1} , respectively, which represent 16-fold and 8-fold improvement compared to the phage enzyme-linked immunosorbent assay. In addition, the P-BLEIA showed good accuracy for the detection of 2,4-D in spiked samples.

*Corresponding Author: Tel.: +86 25 84395479. Fax: +86 25 84395479. huaxiude@njau.edu.cn.

Author Contributions

All authors have given approval to the final version of the manuscript.

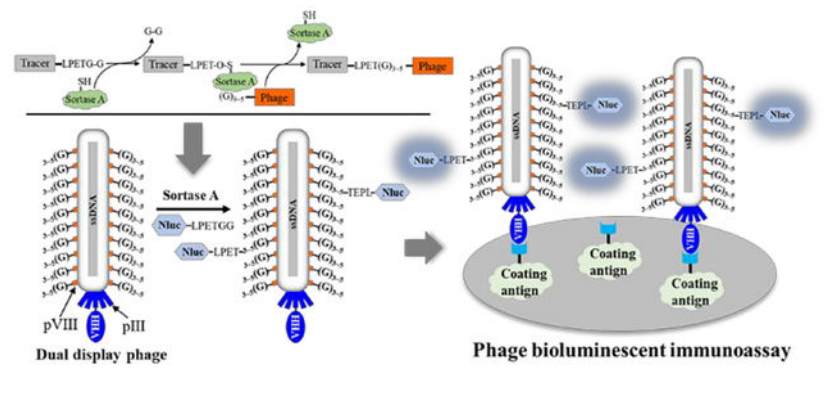
Supporting Information

The primers used in this article; the gene segments for the modification of vectors; the amplification efficiencies of helper phages and dual display phages; the reactivity of five kinds of phage in P-BLEIAs; the luminescence spectrum and bioluminescence kinetics curve of Nluc labeled phage-H.G5; the sensitivities of P-BLEIA for the detection of 2,4-D with different numbers of phage-H.G5; effect of methanol on P-BLEIA; matrix interference on P-BLEIA.

The Supporting Information is available free of charge on the ACS Publications website.

The authors declare no competing financial interest.

Graphical Abstract



Introduction

Phage display technology, especially filamentous phage M13, plays an important role in immunoassay development.¹ There have been many successful reports on the development of immunoassay reagents using phage display libraries, including specific antibodies^{2, 3} and peptides⁴⁻⁶. These affinity ligands can be expressed as recombinant proteins⁷ or directly used as part of phage particles⁸. Depending on the application, the recombinant form of the affinity ligand may offer advantages, as can be the case for the development of lateral flow tests where the reduced size of the protein facilitates homogeneous migration through the membrane.⁹ However, the phage-borne ligand may offer some advantages: a) the target protein is usually displayed in multicopy number, which contributes to an increased avidity,^{10, 11} b) the repetitive structure of the phage characterized by thousands of copies of the main protein pVIII provides a scaffold for a high signal-to-ligand ratio that contributes to increased assay sensitivity,⁹ c) the isolated affinity ligand remains in the same molecular environment that mediates its isolation, thus retaining its maximum activity, and d) very importantly, the isolated phage is in itself the reagent to be used and can be prepared in a simple, standardized way and at low cost. However, its detection relies on the use of secondary antibodies, and it would be desirable to implement simple and efficient methods for direct labeling of the phage to shorten assay steps and facilitate standardization.¹² Chemical labeling of the phage surface has been used for this purpose,^{13, 14} but the different methods require nonphysiological pH, reducing conditions, etc. that may compromise the reactivity of the affinity protein, which can also be affected by the nonspecific derivatization of critical residues.¹⁵

An alternative option to circumvent these hurdles is the use of a mild and specific enzymatic reaction between the peptide tags and tracers, which would be of great benefit to the development of phage immunoassays. This task can be carried out by sortases (Srt), a family of membrane-associated transpeptidases found in Gram-positive bacteria^{16, 17} that have been widely used to covalently fuse polypeptides to the C- and N-termini of proteins. Among them, SrtA from *Staphylococcus aureus*, which recognizes substrates containing the motif of LPXTG (X means any amino acid) of the target protein, can cleave the amide bond between threonine (T) and glycine (G) to yield a reactive acyl-enzyme intermediate

that promotes the ligation of the reactive intermediate with a short polyglycine sequence (G₁₋₅) at the N-terminus of a second partner protein.^{18, 19} The SrtA-mediated reaction occurs specifically and efficiently between proteins that contain the LPXTG motif at the C-terminus and polyglycine at the N-terminus.¹⁷ Interestingly, considering that the reactive tags involved in the SrtA-mediated reaction are remarkably small, their use to modify some of the phage proteins would have minor effects on the phage propagation. Therefore, the SrtA-mediated reaction represents a potential strategy for the labeling of dual display phage.

There are two main ways to display target proteins on the phage surface. One approach uses the phage vector to directly insert the target gene into the phage genome so that each copy of the recombinant capsid protein can display the target protein. This approach can achieve maximum display efficiency but has the strictest size limitation for the displayed protein, so it is usually used to display small peptides.²⁰⁻²² The other approach can be used to display larger proteins based on the combination of phagemid and helper phage.²³ The phagemid contains a gene of capsid protein fused with the target protein and the M13 packing sequence that allows packing the phagemid DNA into progeny phages. The phagemid is unable to generate progeny phages independently until the helper phage supplements the phage protein genes that the phagemid lacks. Hess et al.¹⁵ had used the phage vector system to simultaneously display two small peptide tags on two capsid proteins, and then the tracer and affinity protein were attached to the phage surface using enzyme-mediated reactions. However, for those large proteins (such as antibodies), their system requires cloning and expressing affinity proteins as recombinant proteins, and then attaching them to the phage surface through reactions. It is therefore necessary to construct a dual display system using phagemids that allows direct labeling of phages that display large proteins after isolation.

In this work, we constructed dual display systems (simultaneously displaying polyglycine (G₃ or G₅) on the capsid protein VIII (pVIII) and anti-2,4-dichlorophenoxyacetic acid (2,4-D) VHH on capsid protein III (pIII)) based on the phagemid pComb3XSS. Two variations were explored: a) the fusion of the polyglycine gene with the pVIII gene of helper phage M13KO7 to display high density polyglycine on the phage surface and b) the polycistronic expression in pComb3XSS of the pVIII gene encoding a polyglycine sequence at its N-terminus and the gene of the anti-2,4-D VHH to display a low density of polyglycine modified pVIII on the phage surface. The dual display phages were labeled through the SrtA-mediated reaction with the peptide rhodamine-LPETGG or the protein nanoluciferase (Nluc) containing the sequence LPETGG at its C-terminus (Nluc-LPETGG). The performance of the dual display phages was evaluated, and a phage bioluminescent immunoassay (P-BLEIA) with high sensitivity was developed by employing the dual display phage modified with Nluc.

MATERIALS AND METHODS

Reagents.

Enzymes for vector modification, the M13KO7 vector and anti-pIII antibody were purchased from New England Biolabs (Ipswich, USA). The phagemid pComb3XSS carrying the 2,4-D VHH gene was stored in the laboratory.²⁴ Nluc substrate and pNL1.1 vector were purchased from Promega (Madison, USA). Bacterial protein extraction reagent was

purchased from Thermo Scientific (Waltham, USA). Horseradish peroxidase (HRP)-labeled anti-M13 antibody was purchased from Santa Cruz Biotechnology (Santa Cruz, USA). Anti-His tag antibody was purchased from Tiangen Biochemical Technology (Beijing, China). Genes and primers were synthesized by Genscript Biotech Corporation (Nanjing, China). Rhodamine-LPETGG was prepared by Apeptide Co., Ltd. (Shanghai, China).

Modification of vectors.

Gene segment 1 (Figure S1a), which consisted of the signal peptide pelB, G₃/G₅ and pVIII, was synthesized and digested by *EcoRI*. The digested phagemid pComb3XSS (containing the 2,4-D VHH gene) was ligated with gene segment 1 using T₄ DNA ligase and transferred into ER2738 and named pComb3XSS-VHH-pVIII-G₃ or pComb3XSS-VHH-pVIII-G₅.

Using the M13KO7 vector as a template, primers F_{M1} and R_{M1} (Table S1) were used to amplify the front part of gene segment 2 (Figure S1b), which contained the signal peptide and polyglycine genes. The primers of F_{M2} and R_{M2} (Table S1) were used to amplify the back part, which contained the polyglycine and pVIII genes. The two parts formed the complete gene segment 2 when joined by overlap PCR. Gene segment 2 was cloned into the M13KO7 vector after being digested with *BsrGI* and *BamHI*. The ligation vector was transferred into ER2738 and the products were named M13KO7-pVIII-G₃ or M13KO7-pVIII-G₅.

Phage amplification.

The amplification procedure for helper phages was as follows: ER2738 containing the vector of the helper phage was cultivated in 2 mL 2×YT medium at 37 °C and 250 rpm. When the OD₆₀₀ value reached 0.5, kanamycin at a final concentration of 70 µg mL⁻¹ was added and culture was continued overnight. The supernatant filtered through a 0.22 µm filter membrane was added to an equal volume of glycerin and frozen at -80 °C, which was used as the stock seed. For the large-scale amplification, the stock seed solution was diluted to infect ER2738, then the mixture was cultivated on a culture plate containing 70 µg mL⁻¹ kanamycin, and the plate with 500–1,000 colonies was selected. The colonies were scraped off and transferred to 200 mL 2 × YT medium, and the cultivation procedure was the same as above. The helper phage in the supernatant was precipitated twice with 40 mL 20% PEG8000/2.5 mol L⁻¹ NaCl and resuspended in 1.5 mL 50% glycerin-PBS. After quantifying the phage concentration by UV-vis spectrophotometry,²³ the helper phage stock was stored at -20 °C.

The amplification procedure for dual display phages was as follows: ER2738 containing the phagemid was cultivated in 100 mL 2×YT medium with 100 µg mL⁻¹ ampicillin at 37 °C and 250 rpm until the OD₆₀₀ value reached 0.5. Then 2×10¹² pfu helper phages were added to infect the bacteria at 37 °C for 30 min. After 1 h of shaking at 250 rpm, kanamycin was added to the culture medium at a final concentration of 70 µg mL⁻¹ and cultivated overnight. After precipitation twice by PEG/NaCl, the dual display phage was resuspended in the reaction buffer (50 mmol L⁻¹ Tris-HCl, 150 mmol L⁻¹ NaCl, pH 7.4), and quantified by UV-vis spectrophotometry.

The amplification combinations of different dual display phages are as follows: pComb3XSS-VHH-pVIII-G₃ + M13KO7 for phages with a low density of G₃ (named

phage-L.G₃); pComb3XSS-VHH-pVIII-G₅ + M13KO7 for phages with a low density of G₅ (named phage-L.G₅); pComb3XSS-VHH + M13KO7-pVIII-G₃ for phages with a high density of G₃ (named phage-H.G₃); pComb3XSS-VHH + M13KO7-pVIII-G₅ for phages with a high density of G₅ (named phage-H.G₅); pComb3XSS-VHH + M13KO7 for phages with no polyglycine as a control (named phage-N).

Preparation of proteins.

The pentamutant SrtA²⁶ gene was synthesized and cloned into pET28a within *Nhe* I and *Xho* I, and then the vector was transferred into *E. coli* BL21(DE3) for the expression of SrtA. The gene of Nluc-LPETGG was amplified using F_N and R_N (Table S1) as primers and pNL1.1 as template, which was cloned into pET28a using *Nhe* I and *Xho* I. The expression strain of Nluc-LPETGG was also *E. coli* BL21(DE3). *E. coli* BL21(DE3) cells carrying expression vectors were cultivated in 2×YT medium (containing 70 μg mL⁻¹ kanamycin) at 37 °C and 250 rpm until OD₆₀₀≈0.7. Then, 1 mmol L⁻¹ (final concentration) IPTG was injected to induce the expression of proteins at 20 °C and 250 rpm for overnight. The proteins in the cell cytoplasm were extracted using bacterial protein extraction reagent and purified using a HisTrap column.

SrtA-Mediated Reactions.

For phage-N, phage-L.G₃ and phage-L.G₅, the typical SrtA-mediated reaction (Figure 1a) comprised 4×10¹³ pfu mL⁻¹ phage, 6.4 μmol L⁻¹ SrtA and 64 μmol L⁻¹ rhodamine-LPETGG (or 32 μmol L⁻¹ Nluc-LPETGG) and was incubated for 1 h at 25 °C. For phage-H.G₃ and phage-H.G₅, the reaction comprised 3×10¹³ pfu mL⁻¹ phage, 27 μmol L⁻¹ SrtA and 270 μmol L⁻¹ rhodamine-LPETGG (or 135 μmol L⁻¹ Nluc-LPETGG), incubated for 1 h at 25 °C. SrtA-mediated reactions were carried out in reaction buffer plus 10 mmol L⁻¹ CaCl₂. After the reaction, the mixtures were diluted 200 times and the phages were purified by one PEG/NaCl precipitation.

P-BLEIA.

White opaque microtiter plates (Corning, USA) were coated with 10 μg mL⁻¹ 2,4-D coating antigen at 4 °C overnight (100 μL per well). After five washes with 0.1% Tween-PBS (PBST), the plate was blocked with 5% skim milk-PBS at 37 °C for 2 h. Then 50 μL of Nluc-labeled phage diluted with 5% skim milk-PBST was mixed with 50 μL of 2, 4-D standard or sample solution. The mixture was added to the plate and reacted for 1 h at 37 °C. After 10 washes with PBST, 100 μL PBS containing 0.2 μL Nluc substrate was added, and the luminescence intensity (RLU) was detected by a SpectraMax M5.

Phage enzyme-linked immunosorbent assay (P-ELISA).

The clear microplate (Corning, USA) was coated with 2,4-D coating antigen at 4 °C overnight (10 μg mL⁻¹, 100 μL per well) and subsequently blocked at 37 °C for 2 h with 5% skim milk-PBS. 50 μL phage-N (5×10¹¹ pfu mL⁻¹) and 50 μL of a series of concentrations of 2, 4-D standard solution were added to the plate and reacted for 1 h at 37 °C. After 10 washes with 0.05% Tween 20-PBS, HRP-labeled anti-M13 antibody was added for 1 h incubation to bind with the phages remaining on the plate, and then unreacted reagent was

removed by 10 washes. The TMB substrate (32 μL of 0.75% H_2O_2 and 100 μL of 10 mg mL^{-1} TMB in dimethyl sulfoxide added to 10 mL of 0.02 mol L^{-1} citrate acetate buffer, pH 5.0) was added and incubated for 15 min to determine the amount of phage on the plate. After terminating the reaction with 2 mol L^{-1} H_2SO_4 , the absorbance at 450 nm was detected by a SpectraMax M5 (Molecular Devices, USA).

Cross-Reactivity (CR).

Serial concentrations of standard solutions of 2,4-D analogs (2,4-dichlorotoluene, 2,4-dichlorophenol, phenoxyacetic acid, 2,4-D butyl ester, 2-methyl-4-chloro-phenoxyacetic acid (MCPA), dichlorprop, fenoprop, 2,4,5-trichlorophenoxyacetic acid (2,4,5-T), and 2,4-D methyl ester) were prepared and tested by P-BLEIA to measure the 50% inhibition concentration (IC_{50}) values. The CRs of these analogs were calculated using the following formula: $\text{CR} (\%) = [\text{IC}_{50} (2,4\text{-D})/\text{IC}_{50} (\text{analogs})] \times 100$.

Analysis of spiked samples.

Soil samples were collected from the Nanjing, China area and tomato samples were purchased from a supermarket in Nanjing, China, which were verified by HPLC-MS/MS²⁴ to be free of 2,4-D. The samples were homogenized and spiked with 2,4-D at final concentrations of 20, 60 and 180 ng g^{-1} . The extraction procedure of the samples spiked with 2,4-D was as follows: 10 g spiked samples were accurately weighed and added to 20 mL 50% methanol-PBS. After shaking for 10 min and sonication for 15 min, the extract supernatants were collected using vacuum filtration and adjusted to 25 mL with PBS. The concentrations of 2,4-D in extract supernatants were analyzed by P-BLEIA after appropriate dilution.

Analysis of western blot images.

The western blot images acquired by a multifunctional imager (Vilber, Fusion FX7 IR Spectra) were imported into ImageJ 1.50i software. The images (8-bit type with black background and white bands) were first calibrated using the function "Uncalibrated OD". Then, the horizontal target bands were selected by a rectangular selection tool. After execution of the command "Ctrl+3", a peak plot for selected bands appeared. Subsequently, the straight tool was used to separate the peaks corresponding to each band, and the wand tool was employed to calculate each peak area as the gray intensity for each band.

RESULTS AND DISCUSSION

Construction strategy of dual display systems.

In this work, dual display phages were constructed by displaying polyglycine on pVIII and anti-2,4-D VHH on pIII. Compared with other capsid proteins, using the main capsid protein pVIII (approximately 2700 copies) to display polyglycine can theoretically yield the highest amount of polyglycine on the phage surface theoretically, so that the phage can be coated with more tracers to improve the sensitivity of phage immunoassays. In addition, the reason for using pIII to display VHH was to maintain the original state of the VHH, and phage display VHH libraries are commonly based on a pIII display.

Phagemid-based display involves two vectors: phagemid and helper phage vector. The phagemid carries the fusion fragment of a foreign gene and a capsid protein gene, and the helper phage vector contains all capsid protein genes but lacks the genes for replication and packaging. The pComb3XSS and M13KO7 vectors, which are commonly used phagemid and helper phage, were employed to construct the dual display phage in this work. The 2,4-D VHH was displayed on pIII using the usual method, in which the 2,4-D VHH gene was inserted into the N-terminus of pIII on pComb3XSS. Considering that the simultaneous display of polyglycine may significantly reduce the efficiency of phage amplification, two methods were explored for displaying polyglycine on pVIII at different densities: a) The gene fusion fragment of polyglycine and pVIII was cloned upstream of the VHH gene on pComb3XSS (Figure 1b). This leads to two sources of pVIII for progeny phage assembly: polyglycine-pVIII offered by pComb3XSS and unmodified pVIII offered by the M13KO7 vector, which means that the phage surface is not all polyglycine-pVIII. This approach can display G₃ or G₅ at low density on pVIII, named phage-L.G₃ or phage-L.G₅. b) The polyglycine gene was directly inserted into the N-terminus of pVIII in the M13KO7 vector (Figure 1c). Therefore, the polyglycine-pVIII offered by the M13KO7 vector becomes the single source of pVIII for progeny phage assembly. This approach was accomplished to display G₃ or G₅ at high density on pVIII, named phage-H.G₃ or phage-H.G₅. The unmodified phage that only displayed VHH comes from previous research²⁴ and is named phage-N.

Characteristics of dual display phages.

Considering that there is a lack of the unmodified pVIII gene in the amplification of phage-H.G₃ and phage-H.G₅, the proportions of polyglycine-pVIII in phage-H.G₃ and phage-H.G₅ were supposed to be 100% (~2700 copies). Then, HRP-labeled anti-pVIII antibody was used as the detection antibody to perform the western blot analysis for dual display phages. The results showed that there were no bands in the phage-H.G₃ and phage-H.G₅ lanes (Figure 2a), and it was believed that the polyglycine modification caused the nonrecognition of the anti-pVIII antibody by polyglycine-pVIII. Compared to the same amount of phage-N, the reduction of gray intensity for pVIII bands generated by phage-L.G₃ and phage-L.G₅ was used to evaluate the proportion of polyglycine-pVIII in phage-L.G₃ and phage-L.G₅. A standard curve representing the gray intensity of pVIII bands versus the amount of phage-N particles was established (Figure 2b), which showed that approximately $17.96 \pm 2.17\%$ (~485 ± 59 copies) of pVIII was fused to G₃ in phage-L.G₃, and $6.84 \pm 0.92\%$ (~185 ± 25 copies) of pVIII was fused to G₅ in phage-L.G₅. In addition, an anti-pIII antibody (recognizing the C-terminus of pIII) was used to perform western blot analysis to determine the display efficiency of VHH (Figure 2c). A standard curve was established by plotting the gray intensity of VHH-pIII bands versus the amounts of phage-N (Figure 2d). According to the gray intensity of a known number of other phage particles, the display efficiencies of phage-L.G₃, phage-L.G₅, phage-H.G₃ and phage-H.G₅ were calculated as $105.10 \pm 8.13\%$, $107.25 \pm 10.61\%$, $97.34 \pm 13.77\%$ and $92.82 \pm 12.21\%$ of that of phage-N, respectively. It is believed that the polyglycine moiety essentially does not affect the display efficiency of the VHH on pIII.

Next, we examined the amplification efficiency of the modified phages. Under the same conditions, the amplification efficiencies of M13KO7-G₃ and M13KO7-G₅ were approximately 70% and 50% of that of the M13KO7, respectively (Figure S2a). For dual display phages, there were no significant differences in amplification efficiencies between phage-L.G₃, phage-L.G₅ and phage-N, while the production of phage-H.G₃ and phage-H.G₅ was approximately 60% and 40% lower than that of phage-N, respectively (Figure S2b). As expected, polyglycine fused to pVIII reduced the amplification efficiency of the phages, and the higher the display number and length of the polyglycine moiety, the lower the amplification efficiency. Despite the observed reduction, the production of modified phage is still entirely acceptable for practical use.

SrtA-Mediated Labeling of pVIII.

Once the viability of the polyglycine-modified phages was checked, we initially proceeded to label them by SrtA-mediated conjugation using rhodamine-LPETGG and monitor the reaction by following the fluorescent signals in SDS-PAGE gels. As shown in Figure 3a, the rhodamine-pVIII fluorescent band of (about 6 kDa) was only detected in the presence of phage-H.G₅, StrA and rhodamine-LPETGG, and there was no other fluorescent band indicating that the reaction was highly specific. Next, we analyzed the difference in labeling efficiencies among the four kinds of dual display phages (Figure 3b). A standard curve was established by plotting the fluorescence intensity of rhodamine-pVIII bands versus the amounts of phage-H.G₅ (Figure 3c). According to the fluorescence intensity of a known number of other phage particles, the labeling efficiencies of phage-L.G₃, phage-L.G₅ and phage-H.G₃ were calculated as $7.92 \pm 0.62\%$, $5.81 \pm 0.57\%$ and $53.47 \pm 3.73\%$ of that of phage-H.G₅, respectively. The amount of rhodamine attached to phage-H.G₅ was evaluated according to the fluorescence intensity changes of the reaction solution after labeling. After the phage-H.G₅ was precipitated from the solution, the fluorescence intensities of rhodamine in the reaction solution showed decrease a of $22.92 \pm 1.17\%$, which means that $45.84 \pm 2.34\%$ G₅ (approximately 1238 ± 63 copies) had been labeled with rhodamine. Therefore, approximately there were about 98 ± 8 , 72 ± 7 and 660 ± 46 copies of rhodamine were labeled on phage-L.G₃, phage-L.G₅, and phage-H.G₃, respectively.

We next explored the use of Nluc, a tracer protein with great potential for immunoassay development, for SrtA-mediated labeling of the modified phage. The C-terminus of Nluc was fused to LPETGG, while the N-terminus was equipped with a 6×His tag for purification and western blot analysis. The reaction products under different conditions were analyzed by western blot using an anti-His secondary antibody (Figure 4a). The Nluc-pVIII band (approximately 27 kDa) appeared only when all reactants were present. Then we generated a standard curve by running known amounts of Nluc-LPETGG, which was used to estimate the number of Nluc molecules coupled to each phage modification (Figure 4b and 4c). As expected, phage-H.G₅ yielded the highest labeling number, with 102 ± 16 copies of Nluc per phage, while the labeling numbers of Nluc for phage-L.G₃, phage-L.G₅ and phage-H.G₃ were 33 ± 5 , 28 ± 5 and 77 ± 9 copies, respectively.

The labeling efficiencies reported here were basically the same as those attained by Hess et al.¹⁵, who attached similar molecular size tracers to pVIII using the SrtA-mediated reaction

(50% for biotin-LPETGG and 3.37% for GFP-LPETGG). While there are some simpler chemical conjugation methods that can attain slightly higher labeling efficiency of small molecule tracers to pVIII than the one reported here,^{27, 28} they typically require the use of organic solvents (20% DMSO) and can modify critical residues of the affinity ligand displayed on pIII. In addition to chemical conjugation, the SrtA-mediated binding couples the tracer in an oriented manner.

Sensitivity of P-BLEIA.

Due to its remarkable properties of intense and highly stable luminescence, Nluc has received increasing attention as an immunoassay tracer in recent years.^{6, 9, 29} Interestingly, Nluc-LPETGG can be efficiently produced using *E. coli* expression (approximately 65 mg per liter of culture). This makes it an attractive option for the development of dual display phage-based assays because it is economically much more convenient than using chemically synthesized peptides, such as the rhodamine-LPETGG used in this study. For this reason, the Nluc-labeled dual display phage was used to develop a direct competitive immunoassay (P-BLEIA) for 2,4-D using phage-H.G₅, which generates the highest RLU (RLU_{max}) at the same phage concentrations (Figure S3). The luminescence spectrum of Nluc-labeled phage-H.G₅ was similar to that of Nluc (Figure S4a). In addition, the bioluminescence kinetics curve (Figure S4b) shows that the signal decayed by approximately 8% after 15 minutes, which was sufficiently stable for detection.

To set up the P-BLEIA we initially optimized the amount of phage particles to be used in the test. Similar sensitivities were obtained when the phage concentrations ranged from 2×10^{12} pfu mL⁻¹ to 1.25×10^{11} pfu mL⁻¹. The RLU_{max} was approximately ten times greater than that of the negative control when the phage concentration was greater than or equal to 2.5×10^{11} pfu mL⁻¹ (Figure S5); thus, this concentration was selected. Considering that the extraction and dissolution of the analytes require the use of organic solvents, the tolerance of P-BLEIA to organic solvents was analyzed. When the test was run using different methanol concentrations, the RLU_{max} and 50% inhibition concentration (IC₅₀) were not significantly affected when low methanol concentrations were used (5%), but 10% methanol caused a considerable reduction in RLU_{max} with a moderate reduction in the assay sensitivity (Figure S6).

The standard curves of P-BLEIA and P-ELISA were fitted using the four parameter logistic curve in OriginPro 8.0 (Figure 5). The IC₅₀, limit of detection (LOD, IC₂₀) and linear range (IC₁₀-IC₉₀) of P-BLEIA were 2.15 ng mL⁻¹, 0.491 ng mL⁻¹ and 0.216-18.2 ng mL⁻¹, respectively. Compared to the common P-ELISA (IC₅₀ and LOD of 17.9 ng mL⁻¹ and 7.81 ng mL⁻¹, respectively), the IC₅₀ and LOD of the P-BLEIA were improved 8-fold and 16-fold, respectively. In addition, 2,4-D VHH has been used to develop two colorimetric assays and one fluorometric assay without using phage particles,²⁴ and the sensitivity of the P-BLEIA was better than that of the colorimetric assays (29.2 ng mL⁻¹ and 11.6 ng mL⁻¹) and similar to that of the fluorometric assay (1.9 ng mL⁻¹).

Specificity of P-BLEIA.

The specificity of the P-BLEIA was assessed by studying the cross-reactivities (CRs) with nine 2, 4-D analogs (Table 1). The immunogen for the preparation of 2,4-D VHH exposed the 2,4-chloro-phenoxyacetic acid group, and thus, the only significant CR (14.1%) was found with the MCPA compound. Overall, as expected, the CR results were similar with respect to the specificity of the 2,4-D VHH found with other immunoassays.²⁴

Recoveries.

To study the matrix interference, we used tomato and soil extracts known to be free of 2,4-D. The standard curves of P-BLEIA for extracts with different dilution ratios were developed and compared with 5% methanol-PBS. No major differences were found when the tomato and soil sample extracts were diluted 20-fold (consisting of a 2.5-fold dilution in the extraction procedure, a 4-fold dilution using PBS after extraction and a 2-fold dilution in the P-BLEIA procedure) or more (Figure S7). We then spiked samples with different concentrations of 2,4-D and, after a 20-fold dilution, analyzed them by P-BLEIA. The average recoveries were in the 77.7%–102.6% range (Table 2). The results indicated that the accuracy of the P-BLEIA is satisfactory for the quantitative determination of 2,4-D in the samples.

CONCLUSION

In this work, we modified the pComb3XSS and M13KO7 vectors to construct dual display phages that simultaneously display the anti-2,4-D VHH on pIII and low density (phage-L.G₃ and phage-L.G₅) or high density (phage-H.G₃ and phage-H.G₅) polyglycine on pVIII. Interestingly, even with the highest density and longest length of the polyglycine moiety, the effect on phage amplification was small. Rhodamine-LPETGG and Nluc-LPETGG were then attached to the phage surface by SrtA-mediated reaction to obtain fluorescent and bioluminescent phage particles. The maximum labeling amounts were 1238 ± 63 and 102 ± 16 per phage respectively when phage-H.G₅ was used. The P-BLEIA developed with the Nluc labeled phage-H.G₅ performed with LOD and IC₅₀ value of 0.491 ng mL^{-1} and 2.15 ng mL^{-1} , respectively, which represents an improvement of 16-fold and 8-fold, respectively, compared to the P-ELISA. Meanwhile, the sensitivity of P-BLEIA was not inferior to that of the immunoassays without phage particles.

This work provides a practicable strategy for phage labeling and the development of various phage immunoassays, including: a) Simple preparation of the dual display phage. Notably, after isolating the affinity ligand from the phage display library, the dual display phage with high density polyglycine can be easily obtained by using the modified helper phage for amplification. b) Convenient labeling reaction. SrtA-mediated labeling is performed under mild conditions and is rapid and specific, allowing high labeling efficiency while retaining the reactivity of the pIII display binding protein. Due to the wide range of SrtA-compatible substrates, the dual display phage can be decorated with various tracers (biotin, fluorescent dye, enzyme, etc.) to meet specific needs. c) High sensitivity. The large surface of phage particles and high labeling efficiency contribute to the amplification of the detection signal, improving the sensitivity of the assay. As an increasing number of affinity ligands are being

isolated from phage display libraries, we believe that dual display phages could provide a powerful option for their application.

Supplementary Material

Refer to Web version on PubMed Central for supplementary material.

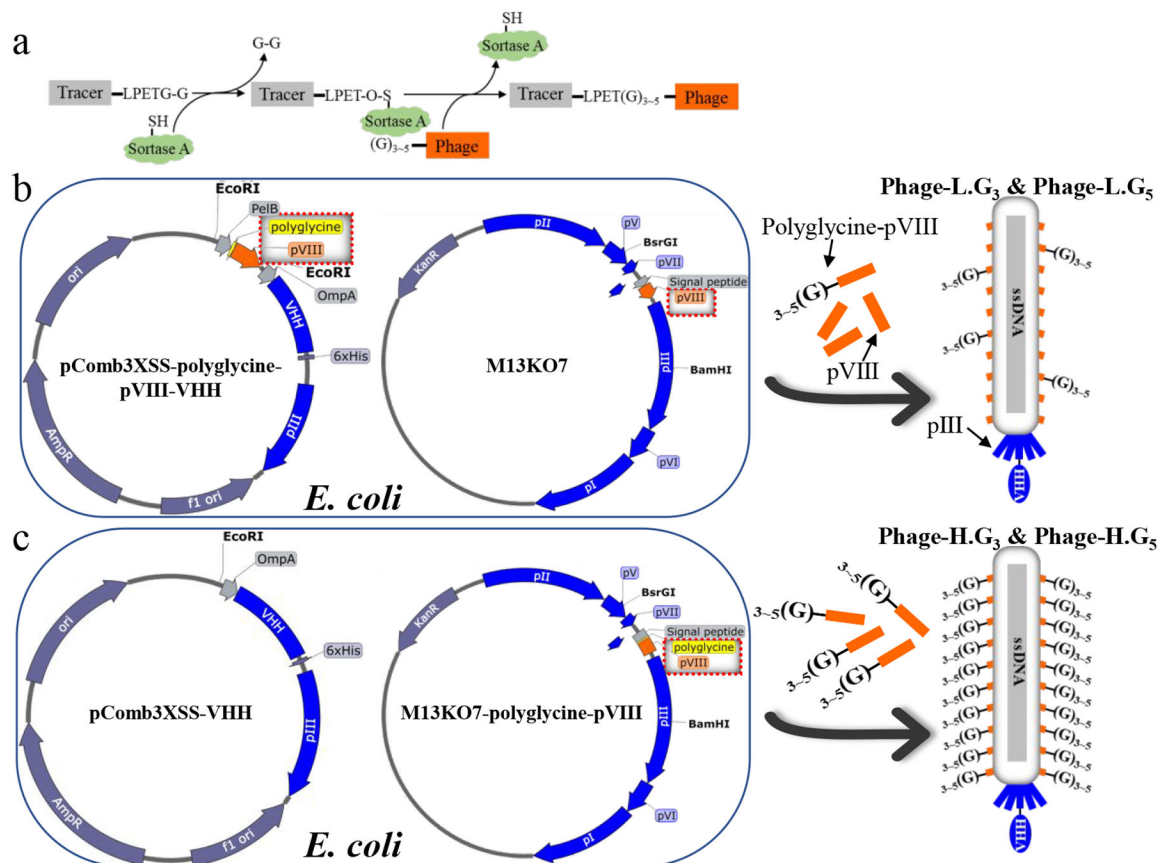
ACKNOWLEDGMENT

This work was supported by the National Natural Science Foundation of China (Grant 31972311), the National Key Research and Development Program of China (Grant 2017YFF0210200). Partial funding was provided by National Institute of Environmental Health Science Superfund Research Program (P42ES004699) and National Institute of Health RIVER Award (R35 ES030443-01).

REFERENCES

- (1). Zhao FC; Shi RR; Liu RX; Tian Y; Yang ZY Application of phage-display developed antibody and antigen substitutes in immunoassays for small molecule contaminants analysis: A mini-review. *Food Chem* 2021, 339, 128084. [PubMed: 33152875]
- (2). Li DY; Cui YL; Morisseau C; Wagner KM; Cho YS; Hammock BD Development of a Highly Sensitive Enzyme-Linked Immunosorbent Assay for Mouse Soluble Epoxide Hydrolase Detection by Combining a Polyclonal Capture Antibody with a Nanobody Tracer. *Anal. Chem* 2020, 92, 11654–11663. [PubMed: 32786492]
- (3). Romao E; Morales-Yanez F; Hu YZ; Crauwels M; De Pauw P; Hassanzadeh GG; Devoogdt N; Ackaert C; Vincke C; Muyldermans S Identification of Useful Nanobodies by Phage Display of Immune Single Domain Libraries Derived from Camelid Heavy Chain Antibodies. *Curr. Pharm. Design* 2016, 22, 6500–6518.
- (4). Hua XD; Yin W; Shi HY; Li M; Wang YR; Wang H; Ye YH; Kim HJ; Gee SJ; Wang MH; Liu FQ; Hammock BD Development of phage immuno-loop-mediated isothermal amplification assays for organophosphorus pesticides in agro-products. *Anal. Chem* 2014, 86, 8441–8447. [PubMed: 25135320]
- (5). Lassabe G; Kramer K; Hammock BD; González-Sapienza G; González-Techera A Noncompetitive Homogeneous Detection of Small Molecules Using Synthetic Nanopeptamer-Based Luminescent Oxygen Channeling. *Anal. Chem* 2018, 90, 6187–6192. [PubMed: 29694028]
- (6). Cardozo S; Gonzalez-Techera A; Last JA; Hammock BD; Kramer K; Gonzalez-Sapienza GG nalyte Peptidomimetics Selected from Phage Display Peptide Libraries: A Systematic Strategy for the Development of Environmental Immunoassays. *Environ. Sci. Technol* 2005, 39, 4234–4241. [PubMed: 15984805]
- (7). Wang F; Li ZF; Yang YY; Wan DB Vasylieva N; Zhang YQ; Cai J; Wang H; Shen YD; Xu ZL; Hammock BD Chemiluminescent Enzyme Immunoassay and Bioluminescent Enzyme Immunoassay for Tenuazonic Acid Mycotoxin by Exploitation of Nanobody and Nanobody-Nanoluciferase Fusion. *Anal. Chem* 2020, 92, 11935–11942. [PubMed: 32702970]
- (8). Liu RX; Shi RR; Zou WT; Chen WH; Yin XC; Zhao FC; Yang ZY Highly sensitive phage-magnetic-chemiluminescent enzyme immunoassay for determination of zearalenone. *Food Chem* 2020, 325, 126905. [PubMed: 32387950]
- (9). Ding Y; Hua XD; Chen H; Liu FQ; Gonzalez-Sapienza G; Wang MH Recombinant peptidomimetic-nano luciferase tracers for sensitive single-step immunodetection of small molecules. *Anal. Chem* 2018, 90, 2230–2237. [PubMed: 29280616]
- (10). Lassabe G; Rossotti M; González-Techera A; González-Sapienza G Shiga-Like Toxin B Subunit of *Escherichia coli* as Scaffold for High-Avidity Display of Anti-immunocomplex Peptides. *Anal. Chem* 2014, 86, 5541–5546. [PubMed: 24797274]
- (11). Chen H; Ding Y; Yang Q; Barnych B; González-Sapienza G; Hammock BD; Wang MH; Hua XD Fluorescent “Turn off-on” Small-Molecule-Monitoring Nanoplatfrom Based on Dendrimer-

- like Peptides as Competitors. *ACS Appl. Mater. Interfaces* 2019, 11, 33380–33389. [PubMed: 31433617]
- (12). Ding Y; Hua XD; Sun NN; Yang JC; Deng JQ; Shi HY; Wang MH Development of a phage chemiluminescent enzyme immunoassay with high sensitivity for the determination of imidaclothiz in agricultural and environmental samples. *Sci. Total. Environ* 2017, 609, 854–860. [PubMed: 28783899]
- (13). Suthiwangcharoen N; Li T; Li K; Thompson P; You S; Wang Q M13 bacteriophage-polymer nanoassemblies as drug delivery vehicles. *Nano Res* 2011, 4, 483–493.
- (14). Jafari MR; Deng L; Kitov PI; Ng S; Matochko WL; Tjhung KF; Zeberoff A; Elias A; Klassen JS; Derda R Discovery of light-responsive ligands through screening of a light-responsive genetically encoded library. *ACS Chem. Biol* 2014, 9,443–450. [PubMed: 24195775]
- (15). Hess GT; Cragolini JJ; Popp MW; Allen MA; Dougan SK; Spooner E; Ploegh HL; Belcher AM; Guimaraes CP M13 Bacteriophage Display Framework That Allows Sortase-Mediated Modification of Surface-Accessible Phage Proteins. *Bioconjugate Chem* 2012, 23, 1478–1487.
- (16). Mazmanian SK; Liu G; Hung TT; Schneewind O Staphylococcus aureus sortase, an enzyme that anchors surface proteins to the cell wall. *Science* 1999, 285, 760–763. [PubMed: 10427003]
- (17). Spirig T; Weiner EM; Clubb RT Sortase enzymes in Gram-positive bacteria. *Mol. Microbiol* 2011, 82, 1044–1059. [PubMed: 22026821]
- (18). Ton-That H; Liu G; Mazmanian SK; Faull KF; Schneewind O Purification and characterization of sortase, the transpeptidase that cleaves surface proteins of Staphylococcus aureus at the LPXTG motif. *P. Natl. Acad. Sci. U.S.A* 1999, 96, 12424–12429.
- (19). Ilangovan U; Ton-That H; Iwahara J; Schneewind O; Clubb RT Structure of sortase, the transpeptidase that anchors proteins to the cell wall of Staphylococcus aureus. *P. Natl. Acad. Sci. U.S.A* 2001, 98, 6056–6061.
- (20). Kretzschmar T; Geiser M Evaluation of antibodies fused to minor coat protein III and major coat protein VIII of bacteriophage M13. *Gene* 1995, 155, 61–65. [PubMed: 7698668]
- (21). Greenwood J; Willis AE; Perham RN Multiple display of foreign peptides on a filamentous bacteriophage. Peptides from Plasmodium falciparum circumsporozoite protein as antigens. *J. Mol. Biol* 1991, 220, 821–827. [PubMed: 1880799]
- (22). Iannolo G; Minenkova O; Petruzzelli R; Cesareni G Modifying filamentous phage capsid: limits in the size of the major capsid protein. *J. Mol. Biol* 1995, 248, 835–844. [PubMed: 7752244]
- (23). Qi H; Lu HQ; Qiu HJ; Petrenko V; Liu AH Phagemid Vectors for Phage Display: Properties, Characteristics and Construction. *J. Mol. Biol* 2012, 417, 129–143. [PubMed: 22310045]
- (24). Li ZF; Dong JX; Vasylieva N; Cui YL; Wan DB; Hua XD; Huo JQ; Yang DC; Gee SJ; Hammock BD Highly specific nanobody against herbicide 2,4-dichlorophenoxyacetic acid for monitoring of its contamination in environmental water. *Sci. Total. Environ* 2021, 753, 141750.
- (25). Barbas CF, Burton DR, Scott JK, Silverman GJ Phage Display: A Laboratory Manual, 2001, Cold Spring Harbor Laboratory Press, Cold Spring Harbor, NY.
- (26). Chen I; Dorr BM; Liu DR A general strategy for the evolution of bond-forming enzymes using yeast display. *P. Natl. Acad. Sci. U.S.A* 2011, 108, 11399–11404.
- (27). Li K; Chen Y; Li SQ; Huong GN; Niu ZW; You SJ; Mello CM; Lu XB; Wang QA Chemical modification of M13 bacteriophage and its application in cancer cell imaging. *Bioconjug. Chem* 2010, 21, 1369–1377. [PubMed: 20499838]
- (28). Niu Z; Bruckman M; Harp B; Mello C; Wang Q Bacteriophage M13 as a Scaffold for Preparing Conductive Polymeric Composite Fibers. *Nano Res* 2008, 1, 235–241.
- (29). Eom S; Bae Y; Kim S; Choi H; Park J; Kang S Development of Recombinant Immunoglobulin G-Binding Luciferase-Based Signal Amplifiers in Immunoassays. *Anal. Chem* 2020, 92, 5473–5481. [PubMed: 32142265]

**Figure 1.**

The schemes of SrtA-Mediated labeling and dual display phage's preparation. (a) The mechanism of SrtA-mediated labeling to phage. (b) The modified pComb3XSS-polyglycine-pVIII-VHH phagemid combined with M13KO7 vector for preparation of phage-L.G₃ and phage-L.G₅. (c) The modified M13KO7-polyglycine-pVIII vector combined with pComb3XSS-VHH phagemid for preparation of phage-H.G₃ and phage-H.G₅.

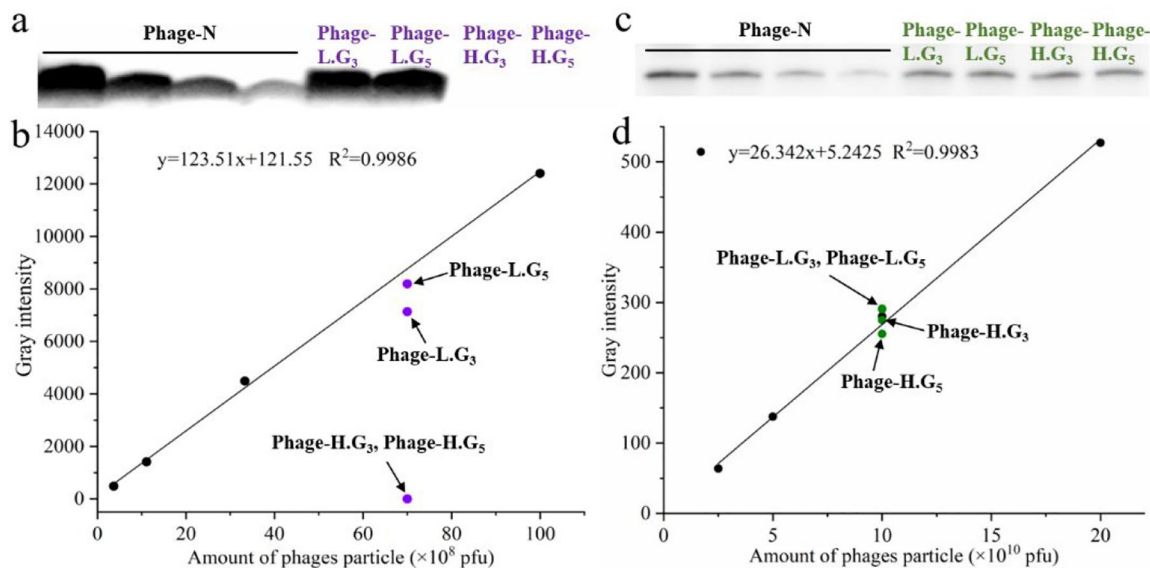
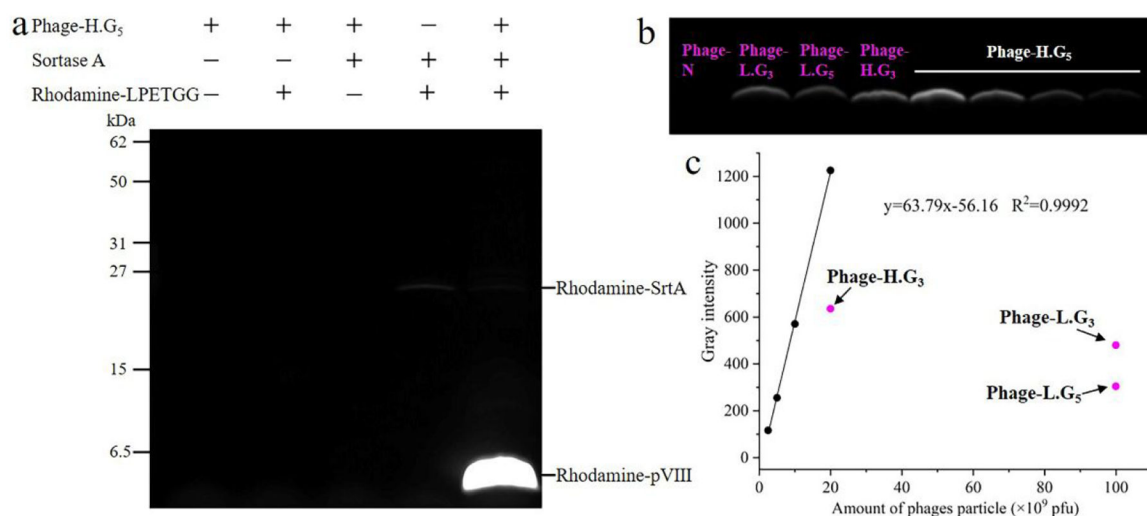


Figure 2.

Western blot analysis of pIII and pVIII in different dual display phages. (a) Western blot bands obtained with the anti-pVIII antibody. (b) Standard curve (black line) representing the relationship between the gray intensity of the pVIII band and the amount of phage-N particles. The purple dots represent the gray intensity generated by 7×10^9 pfu of the various forms of dual display phage. (c) Western blot bands obtained with the anti-pIII antibody. (d) Standard curve (black line) representing the relationship between the gray intensity of the VHH-pIII band and the amount of phage-N particles. The green dots represent the gray intensity generated by 1×10^{11} pfu of the various forms of dual display phage.

**Figure 3.**

Gel analysis of SrtA-mediated rhodamine labeling. (a) SDS-PAGE of the coupling reaction with different components; (b) SDS-PAGE gel showing the relative amount of rhodamine coupled to pVIII on different dual display phages; (c) Standard curve (black line) showing the fluorescence intensity of rhodamine-pVIII bands (gray intensity) versus the amount of phage-H.G₅. The magenta dots represent the fluorescence intensity generated by 2×10^{10} pfu phage-H.G₃, 1×10^{11} pfu phage-L.G₃ and 1×10^{11} pfu phage-L.G₅.

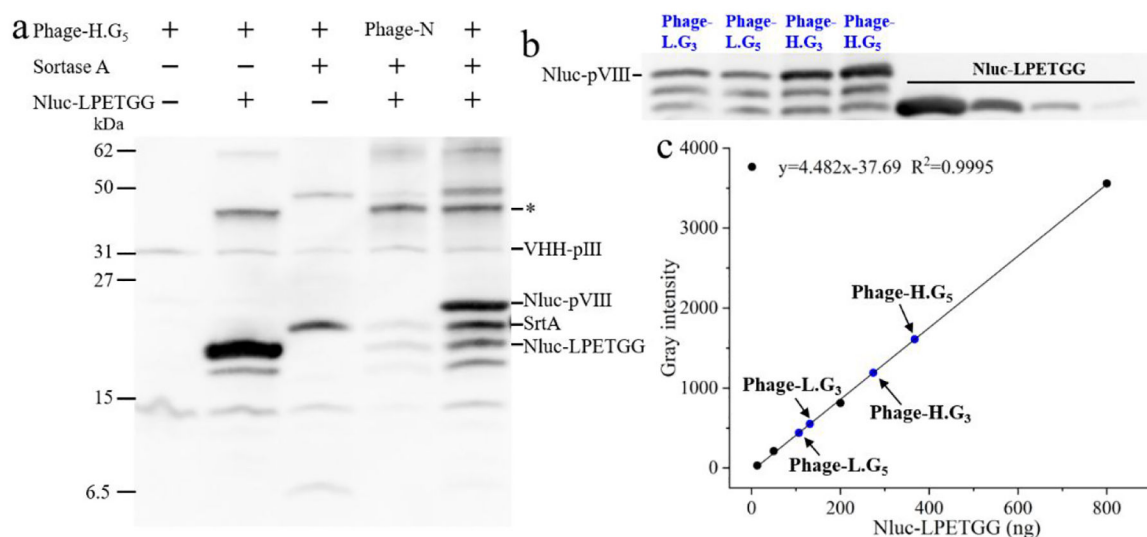


Figure 4.

Western blot analysis of the SrtA-mediated Nluc labeling using the anti-His antibody (Nluc-LPETGG was equipped a His tag at N terminal and SrtA was equipped the His tags at N terminal and C terminal). (a) Western blot of the coupling reaction with different components. Considering that the relative molecular mass of Nluc is 22.6 kDa, the unidentified anti-His tag reactive protein (*) is most probably the dimer of Nluc. (b) Western blot showing the relative amount of Nluc coupled to pVIII on different dual display phages. (c) Standard curve (black line) showing the gray intensity analysis of the Nluc bands versus the amount of Nluc. The blue dots correspond to the gray intensity generated by 1×10^{11} pfu dual display phages and the amount of Nluc they carried.

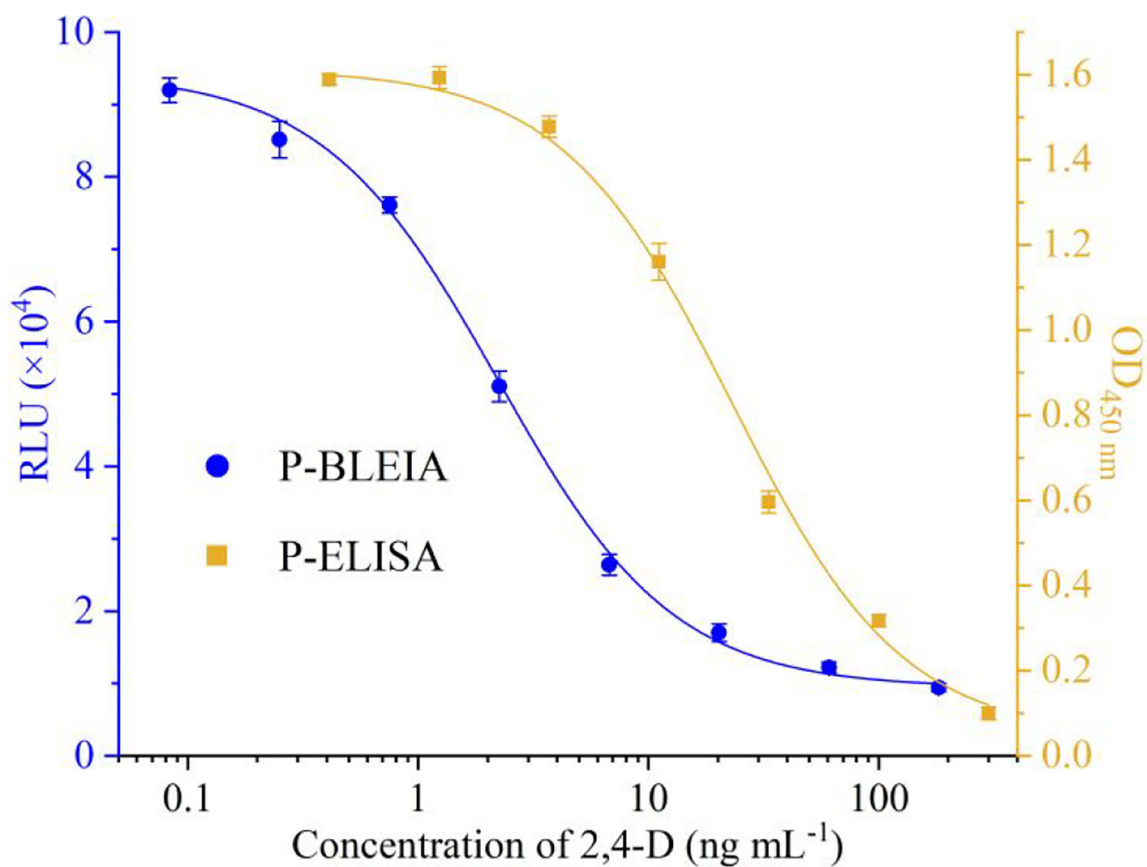


Figure 5. Standard curve for the measurement of 2,4-D by P-BLEIA and P-ELISA. Serial dilutions of 2,4-D standard were mixed with an optimized amount of phage (phage-H.G₅ for P-BLEIA, phage-N for P-ELISA) and then 100 μ L of the mixtures were added to the 2,4-D antigen-coated wells. Each point represents the mean value of three replicates.

Table 1.

Cross-Reactivities of a Set of Analogs Structurally Related to 2,4-D by P-BLEIA

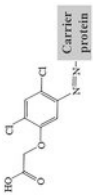
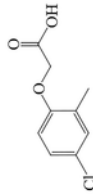
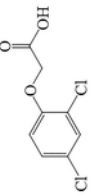
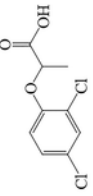
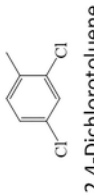
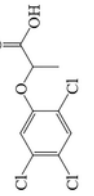
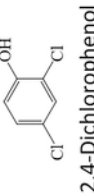
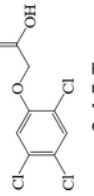
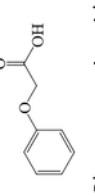
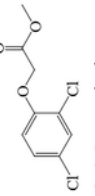
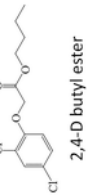
Compound	IC ₅₀ (ng mL ⁻¹)	CR (%)	Compound	IC ₅₀ (ng mL ⁻¹)	CR (%)
 Carrier protein Immunogen	---	---	 MCPA	15.3	14.1
 2,4-D	2.15	100	 Dichlorprop	710	0.3
 2,4-Dichlorotoluene	>2400	<0.1	 Fenoprop	638	0.3
 2,4-Dichlorophenol	>2400	<0.1	 2,4,5-T	922	0.2
 Phenoxyacetic acid	>2400	<0.1	 2,4-D methyl ester	217	1.0
 2,4-D butyl ester	259	0.8			

Table 2.Average Recoveries of 2,4-D Spiked into Environmental and Agricultural Samples ($n=3$)

Sample	Spiked (ng g ⁻¹)	Measured \pm SD (ng g ⁻¹)	Average recovery (%)	RSD (%)
Soil	20	15.5 \pm 1.34	77.7	8.7
	60	61.6 \pm 6.15	102.6	10.0
	180	165 \pm 12.8	91.5	7.8
Tomato	20	17.5 \pm 0.790	87.6	4.6
	60	47.5 \pm 2.84	79.2	6.0
	180	163 \pm 14.4	90.4	8.9